ORIGINAL ARTICLE

AASLD
AMERICAN ASSOCIATION FOR
THE STUDY OF LIVER DISEASES

Switch-associated protein 70 protects against nonalcoholic fatty liver disease through suppression of TAK1

Qiaofeng Qian[1] | **Yang Li**[1] | **Jiajun Fu**[2] | **Dewen Leng**[1] | **Zhe Dong**[1] | **Jiajun Shi**[1] | **Hongjie Shi**[1] | **Dengwei Cao**[1] | **Xu Cheng**[3] | **Yufeng Hu**[2] | **Qiujie Luo**[1] | **Manli Hu**[2] | **Yong Ran**[1] | **Hao Tang**[1] | **Hui Liu**[3,4] | **Jinping Liu**[1]

[1]Department of Cardiovascular Surgery, Zhongnan Hospital of Wuhan University, Wuhan, China

[2]Medical Science Research Centre, Zhongnan Hospital of Wuhan University, Wuhan, China

[3]Department of Cardiology, Renmin Hospital of Wuhan University, Wuhan, China

[4]Institute of Model Animal of Wuhan University, Wuhan, China

Correspondence
Jinping Liu, Department of Cardiovascular Surgery, Zhongnan Hospital of Wuhan University, 169 Donghu Road, Wuhan 430071, China.
Email: liujinping@znhospital.cn

Hui Liu, Institute of Model Animal of Wuhan University, 169 Donghu Road, Wuhan 430071, China.
Email: liuhui86@whu.edu.cn

Abstract

Background and Aims: NAFLD is a progressive disease without known effective drug treatments. Switch-associated protein 70 (SWAP70) is a guanine nucleotide exchange factor that participates in the regulation of many cellular processes. However, the role of SWAP70 in NAFLD remains unclear. This study aimed to identify the function and mechanism of SWAP70 in NAFLD.

Approach and Results: The results showed that the expression of SWAP70 was significantly increased in mice and hepatocytes after metabolic stimulation. Overexpression of *SWAP70* in hepatocytes suppressed lipid deposition and inflammation, and *SWAP70* knockdown created the inverse effect. Using hepatocyte-specific *Swap70* knockout and overexpression mice fed a high-fat, high-cholesterol diet, we demonstrated that SWAP70 suppressed the progression of nonalcoholic steatohepatitis by inhibiting lipid accumulation, inflammatory response, and fibrosis. Mechanically, RNA sequencing analysis and immunoprecipitation assays revealed that SWAP70 inhibited the interaction between transforming growth factor β-activated kinase 1 (TAK1) binding protein 1 and TAK1 and sequentially suppressed the phosphorylation of TAK1 and subsequent c-Jun N-terminal kinase/P38 signaling. Inhibition of TAK1 activation blocked hepatocyte lipid deposition and inflammation caused by *SWAP70* knockdown.

Abbreviations: 5Z-7ox, 5Z-7oxozeaenol; aa, amino acid; ALT, alanine aminotransferase; AST, aspartate aminotransferase; CCL2, chemokine (C-C motif) ligand 2; Cxcl10, chemokine (C-X-C motif) ligand 10; CPT1A, carnitine palmitoyltransferase 1A; DEG, differentially expressed gene; FBG, fasting blood glucose; GST, glutathione S-transferase; GTT, glucose tolerance test; H&E, hematoxylin and eosin; HEK, human embryonic kidney; HFD, high-fat diet; HFHC, high-fat, high-cholesterol; HKO, hepatocyte-specific knockout; ITT, insulin tolerance test; JNK, c-Jun N-terminal kinase; LDL-C, LDL cholesterol; MAPK, mitogen-activated protein kinase; MEKK, mitogen-activated protein kinase kinase kinase; HA, influenza hemagglutinin epitope (YPYDVPDYA); OE, overexpression; PA, palmitic acid; PO, palmitic acid plus oleic acid; PPARA, peroxisome proliferator-activated receptor alpha; PPARG, peroxisome proliferator-activated receptor gamma; RNA-seq, RNA sequencing; SCD1, stearoyl-coenzyme A desaturase 1; SWAP70, switch-associated protein 70; TAB, TAK1 binding protein; TAK1, transforming growth factor β-activated kinase 1; TC, total cholesterol; TG, triglyceride.

Qiaofeng Qian, Yang Li, and Jiajun Fu are contributed equally to this work.

Conclusions: SWAP70 is a protective molecule that can suppress the progression of NAFLD by inhibiting hepatic steatosis and inflammation. SWAP70 may be important for mitigating the progression of NAFLD.

INTRODUCTION

With increased worldwide prevalence of obesity, associated metabolic syndrome and its manifestations, including NAFLD, have increased rapidly. NAFLD is now the most common chronic disease in the liver, affecting 25% of the global population.[1,2] NAFLD is a progressive disease characterized by persistent liver dysfunction, including steatosis, inflammation, and fibrosis, accompanied by continuous injury that ultimately leads to liver cirrhosis and hepatocellular carcinoma.[3] According to its pathological conditions, NAFLD can be divided into nonalcoholic fatty liver and NASH, with the latter becoming the main cause of liver transplants among adults in Europe and the United States.[4] China also exhibits high annual incidence, prevalence, and mortality rates of NAFLD.[5,6] Moreover, NAFLD is a strong inducer of cardiovascular events and increases cardiovascular risk and mortality.[7-9] The gradual increase in the prevalence of NAFLD and the absence of effective drug interventions have prompted investigators to explore effective drug targets for NAFLD.

As one of the two members of the SWEF family, switch-associated protein 70 (SWAP70) is a phosphatidylinositol 3,4,5-trisphosphate-dependent guanine nucleotide exchange factor with a unique arrangement of domains: an exchange factor hand, a pleckstrin-homology domain, a Dbl homology domain, and a C-terminal actin-binging site from the N-terminus to the C-terminus. Relying on actin cytoskeleton binding and regulation, SWAP70 widely participates in cell migration, adhesion, phagocytosis, and morphogenesis.[10-12] For instance, SWAP70 is associated with the formation of cell shape in activated B lymphocytes, the differentiation and migration of dendritic cells, and the migration and invasion of tumor cells.[13-16] SWAP70 has been reported to be related to the regulation of osteoclast function,[17] and is also involved in immune regulation, including maturation and differentiation of immune cells.[15-18] SWAP70 deficiency can lead to an imbalance in the immune environment and enhance inflammatory responses in the body.[19] However, the function of SWAP70 in NAFLD remains unknown.

In the current study, we found that the expression of SWAP70 was significantly increased during the development of NAFLD. Cellular knockdown of *SWAP70* and genetic depletion of *Swap70* in the liver aggravated lipid accumulation and inflammation, ultimately leading to the progression of NAFLD. Moreover, RNA sequencing (RNA-seq) analysis verified that the mitogen-activated protein kinase (MAPK) pathway was the most significantly changed in mice model. We further explored the upstream molecules of MAPK pathway and identified that SWAP70 interacted with transforming growth factor β-activated kinase 1 (TAK1). Mechanically, we found that SWAP70 inhibited the interaction of TAK1 binding protein (TAB) 1 and TAK1, thus suppressing activation of TAK1 and downstream c-Jun N-terminal kinase (JNK)/P38 pathway. More importantly, the regulation of SWAP70 in hepatocyte lipid accumulation and inflammation was dependent on TAK1 activity. Inhibition of TAK1 activity blocked hepatocyte lipid deposition and inflammation caused by *SWAP70* knockdown. This study revealed that SWAP70 protected against NAFLD by inhibiting TAK1 activity, and SWAP70 may be served as a therapeutic target for NAFLD.

MATERIALS AND METHODS

Animal experiments

C57BL/6J mice were fed high-fat diet (HFD) for 24 weeks or fed a high-fat, high-cholesterol (HFHC) diet for 16 weeks to establish a fatty liver model or NASH model, respectively. Mice from the control group were provided commercial feed. All animals were received humane care according to the Guide from the Care and Use of Laboratory Animals published by the National Institutes of Health, and the animal experiments were approved by the Institutional Animal Care and Use Committee of the Renmin Hospital of Wuhan University.

Human liver samples

Human liver samples were collected from individuals who underwent laparoscopic vertical banded gastroplasty for excessive obesity and hepatic surgery at the Renmin Hospital and Zhongnan Hospital of Wuhan University. All human samples were obtained with written informed consent from the patients or their relatives and after the authorization of the Hospital Committee for Investigation in Humans and no donor organs were obtained from executed prisoners or other institutionalized person. All human studies followed the principles of the Declaration of Helsinki.

Primary hepatocytes

Primary hepatocytes were obtained using a two-step collagenase perfusion method as previously described.[20] Detailed methods are listed in the Supporting Information.

Cell lines

L02, human embryonic kidney (HEK) 293, and 293T cell lines were obtained from the Type Culture Collection of the Chinese Academy of Science. A detailed description is stated in the Supporting Information.

Generation of genetically modified mice

Hepatocyte-specific *Swap70*-knockout (*Swap70*-HKO) mice were generated by mating *SWAP70*$^{fl/fl}$ mice with albumin-Cre transgenic mice. To generate *SWAP70* overexpression (*SWAP70*-OE) mice, a Sleeping Beauty transposase system was used. The generation details are displayed in the Supporting Information.

Western blot analysis

Western blot is employed to detect the expression level of indicated proteins, and detailed methods are displayed in the Supporting Information.

Real-time PCR

The mRNA level was detected by real-time PCR, and detailed methods are displayed in the Supporting Information.

Mouse metabolic and liver function assays

The fasting blood glucose (FBG) levels and body weights of the mice were measured every 4 weeks. After 24 weeks of HFD feeding or 16 weeks of HFHC diet, liver weights of mouse models were assessed. Insulin tolerance test (ITT) and glucose tolerance test (GTT) assays were measured at indicated time. Hepatic triglycerides (TG) level was measured by commercial kits. Serum TG, total cholesterol (TC), LDL cholesterol (LDL-C), alanine aminotransferase (ALT), and aspartate aminotransferase (AST) levels were measured using an ADVIA 2400 Chemistry System Analyzer.

Histopathology

The details of histopathological experiments are displayed in the Supporting Information.

Immunofluorescence

The details of immunofluorescent experiments are described in the Supporting Information.

Confocal

HEK 293T cells were infected with influenza hemagglutinin epitope (YPYDVPDYA) tagged *SWAP70* (HA-*SWAP70*) and Flag-*TAK1* plasmids and incubated with corresponding primary and secondary antibodies. Cells for Nile red staining were stained with 1 μM Nile red. Images were obtained using a confocal laser-scanning microscope. The detailed methods are performed in the Supporting Information.

Intracellular TG measurement

TG content was measured using a commercial kit according to the manufacturer's instructions.

Plasmid construction and viral infection

The detailed description about the plasmid construction and viral infection is stated in the Supporting Information.

Immunoprecipitation assays

HEK 293T cells transfected with the indicated plasmids were lysed and incubated with protein A/G agarose beads. After washing with 300 mM and 150 mM NaCl buffer, beads were boiled and the samples were subjected to western blot analysis. The detailed methods are performed in the Supporting Information.

Glutathione *S*-transferase precipitation assays

HEK 293T cells were collected after transfection with glutathione *S*-transferase (GST)-HA–tagged protein or Flag-tagged protein and incubated together as indicated. Then, beads were washed with washing buffer and boiled for 10 min at 95°C. Finally, the samples were subjected to western blot analysis. The detailed method is performed in the Supporting Information.

RNA-seq and analysis

A complementary DNA library was established with the improved RNA, and then the single-ended library was sequenced using MGISEQ-2000. The detailed methods are performed in the Supporting Information.

Statistical analysis

All analyses were performed using SPSS software. The Student *t* test and Mann-Whitney U test were used

to evaluate differences between two groups. One-way ANOVA was used to compare multiple groups. For data with homogeneity or heterogeneity of variance, the Bonferroni post hoc test or Tamhane T2 post hoc test was applied, respectively. When data met a nonnormal distribution, a Kruskal-Wallis nonparametric statistical test was used. All data are expressed as mean ± SD. Differences were considered statistically significant at $p < 0.05$.
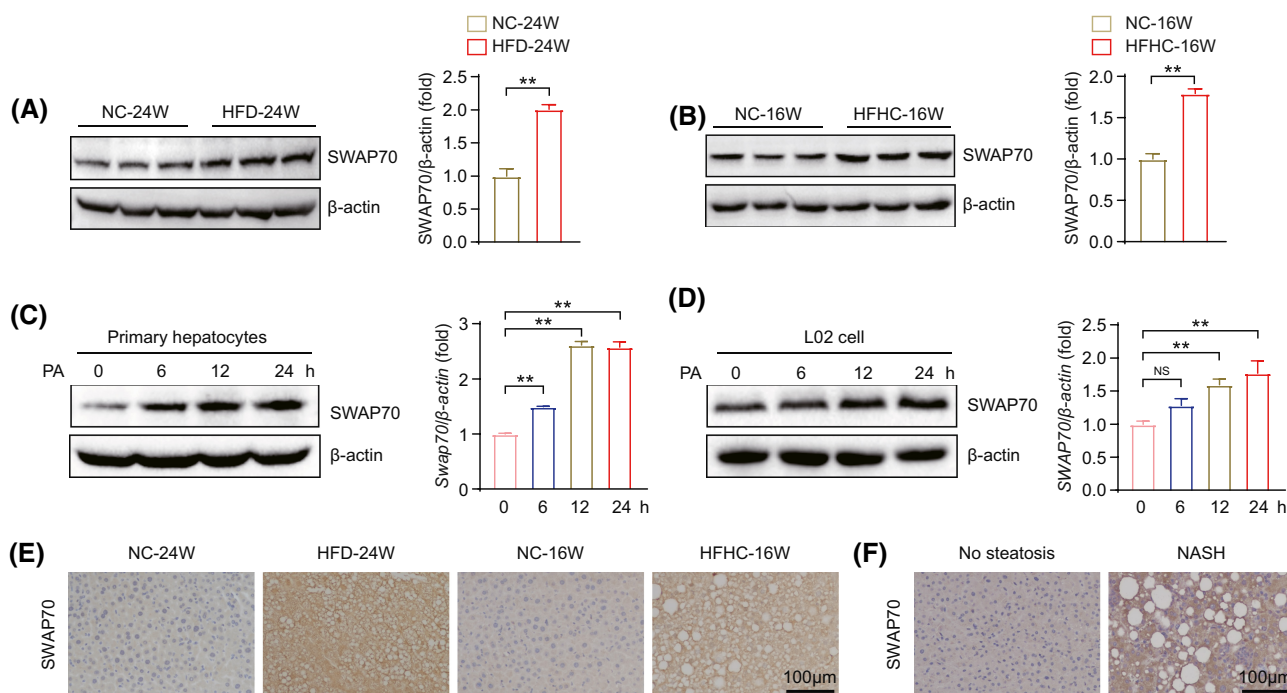
RESULTS

SWAP70 expression is increased in livers and hepatocytes under metabolic challenge

To investigate whether SWAP70 was involved in the pathogenesis of NAFLD, we first detected SWAP70 expression in mouse livers after HFD or HFHC treatment. The results showed that the protein levels of SWAP70 were significantly higher in mice with HFD or HFHC treatment than those in mice fed the normal chow diet (Figure 1A,B). In accordance with these results, the

protein expression of SWAP70 was also increased in both primary mouse hepatocytes and L02 cells after stimulation with palmitic acid (PA) (Figure 1C,D). However, *in vivo* and *in vitro* experiments showed that the mRNA expression level of *SWAP70* did not significantly change, indicating a posttranslational modification of SWAP70 in response to metabolic stimulation (Figure S1). Furthermore, immunohistochemical staining confirmed that the expression of SWAP70 was up-regulated in the livers of mice after HFD or HFHC treatment as well as in individuals with NASH (Figure 1E,F). These findings demonstrate that SWAP70 expression is significantly increased in livers and hepatocytes after metabolic stimulation and may play an important role in the development of NAFLD.

SWAP70 suppresses lipid accumulation and inflammation in hepatocytes after metabolic stimulation

We established *SWAP70*-overexpressing (*SWAP70*-OE) L02 cells and verified them by western blotting (Figure 2A). Compared with the control group, SWAP70-OE significantly

FIGURE 1   SWAP70 expression is increased in livers and hepatocytes under metabolic challenge. (A) Protein expression of SWAP70 in mouse livers after 24 weeks of normal chow (NC) or HFD treatment (*n* = 3/group); bar chart shows quantitative result. (B) Protein expression of SWAP70 in mouse livers after 16 weeks of NC or HFHC diet treatment (*n* = 3/group); quantitative result shown on the right side. (C) Western blotting of SWAP70 in mouse primary hepatocytes after stimulation with PA for 0, 6, 12, and 24 hours (*n* = 3 independent experiments). Quantitative result shown on the right side. (D) Western blotting of SWAP70 in L02 cells after stimulation with PA for 0, 6, 12, and 24 hours (*n* = 3 independent experiments). Quantitative result shown on the right side. (E) Representative immunohistochemical staining images of SWAP70 expression in mouse livers after HFD or HFHC diet for 24 or 16 weeks, respectively (*n* = 5/group). (F) Representative immunohistochemical staining images of SWAP70 in human liver tissues with no steatosis or NASH (*n* = 10-11/group). Scale bar, 100 µm. All data are shown as mean ± SD. The protein expression of target genes was normalized by the expression of β-Actin. Student *t* test (A,B,G,H) or one-way ANOVA (C,D,I,J) with Bonferroni's post hoc analysis or with Tamhane T2 post hoc test was used. ***p* < 0.01
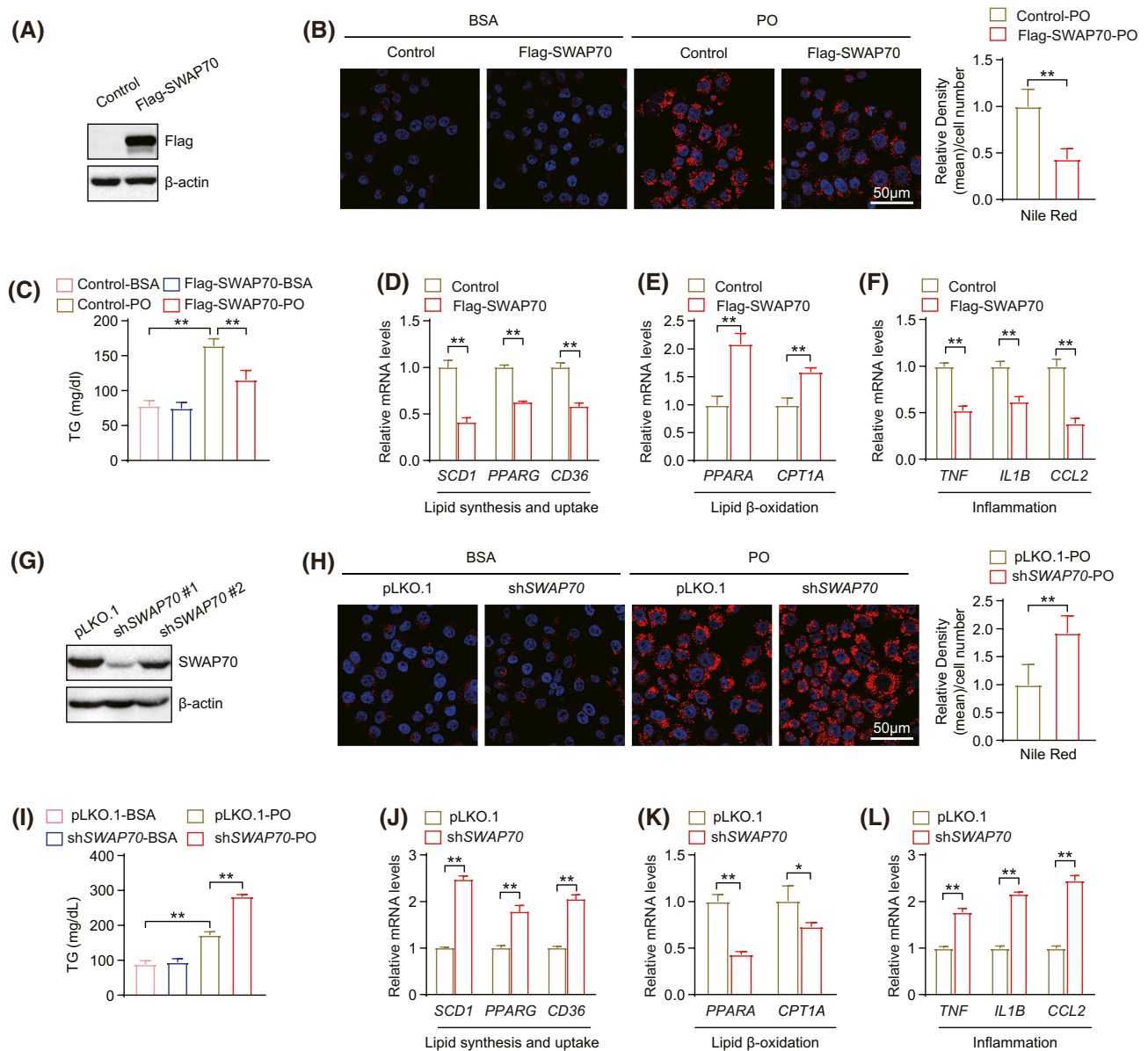
FIGURE 2 SWAP70 suppresses lipid accumulation and inflammation in hepatocytes after metabolic stimulation. (A) The SWAP70 protein expression in L02 cells infected with Control or Flag-*SWAP70* lentivirus. (B) Representative Nile Red staining images showing lipid accumulation in L02 cells followed by bovine serum albumin (BSA) or PO treatment for 12 hours. Scale bar, 50 μm (*n* = 3 independent experiments). (C) Intracellular TG level in the indicated groups (*n* = 3/group). (D-F) Relative mRNA levels of genes related to lipid synthesis (*SCD1*, CD36 molecule [*CD36*], *PPARG*), steatolysis (*PPARA*, carnitine palmitoyltransferase 1A [*CPT1A*]), and inflammation (*TNF*, *IL-1B*, *CCL2*) in L02 cells with BSA or PA stimulation in Control or *SWAP70*-OE (Flag-*SWAP70*) group (*n* = 3 independent experiments). (G) Protein expression level of SWAP70 in L02 cells infected with pLKO.1, sh*SWAP70* #1, and sh*SWAP70* #2 lentivirus. sh*SWAP70* #1 was used for further study. (H,I) Representative Nile Red staining images and relative intracellular TG levels (I) were assessed in L02 cells infected with pLKO.1 or sh*SWAP70* lentivirus after BSA or PO treatment. Scale bar, 50 μm (*n* = 3/group). (J-L) Bar graph shows the relative mRNA levels of genes related to lipid accumulation (J), steatolysis (K), and inflammation (L) in the indicated groups (*n* = 3 independent experiments). All data are shown as mean ± SD. Student *t* test (B,D-H,J-L) or one-way ANOVA (C,I) with Bonferroni's post hoc analysis or with Tamhane T2 post hoc test was used. *$p < 0.05$; **$p < 0.01$

reduced lipid accumulation in response to palmitic acid plus oleic acid (PO) stimulation (Figure 2B). Consistently, the cellular TG content was also lower in the *SWAP70*-OE group than in the control group (Figure 2C). Additionally, the elevated expression of *SWAP70* suppressed the expression of genes related to fatty acid uptake and synthesis (stearoyl-coenzyme A desaturase 1 [*SCD1*], peroxisome proliferator-activated receptor gamma [*PPARG*], and CD36 molecule [*CD36*]) and promoted the expression of genes related to β-oxidation (peroxisome proliferator-activated receptor alpha [*PPARA*], carnitine palmitoyltransferase 1A [*CPT1A*]) (Figure 2D,E). Moreover, *SWAP70*-OE alleviated the inflammatory reaction in hepatocytes under metabolic challenge, as indicated by the down-regulation of proinflammatory genes (*TNF*, *IL-1B*, chemokine [C-C motif] ligand 2 [*CCL2*]) (Figure 2F). We further investigated

the effect of *SWAP70* knockdown on hepatocytes lipid accumulation and inflammatory response. The results showed that *SWAP70* knockdown promoted lipid accumulation in hepatocytes (Figure 2G-I). The expression of genes related to lipid accumulation and inflammation was significantly increased in *SWAP70* knockdown hepatocytes, whereas the expression of genes related to β oxidation was decreased (Figure 2J-L). Furthermore, consistent results were obtained in primary hepatocytes (Supporting Figure S2). Collectively, these results demonstrate that SWAP70 suppresses hepatocytes lipid accumulation and inflammatory responses under metabolic stimulation.

Hepatocyte-specific SWAP70 deficiency exacerbates HFD-induced NAFLD progression

To further define the effect of hepatic SWAP70 on the pathogenesis of NAFLD *in vivo*, we established hepatocyte-specific *Swap70*-knockout (*Swap70*-HKO) mice, and Flox mice were used as the control group (Supporting Figure S3A-C). After 24 weeks of HFD feeding, the body weights showed no significant changes between the *Swap70*-HKO and Flox groups (Supporting Figure S3D). However, compared with the Flox group, *Swap70*-HKO mice exhibited higher FBG levels (Figure 3A), GTT (Figure 3B), and ITT (Figure 3C) results. Moreover, under metabolic stimulation, *Swap70*-HKO mice gained more liver weight, higher liver to body weight ratio and TG levels in hepatic tissues than control mice (Figure 3D-F). Additionally, we measured the levels of circulating TG, TC, and LDL-C in the blood and found that *Swap70*-HKO mice exhibited higher lipid content than control mice (Figure 3G). Representative hematoxylin and eosin (H&E) and Oil Red O staining showed severe lipid accumulation in the livers of *Swap70*-HKO mice compared with Flox mice (Figure 3H). Consistently, *Swap70*-HKO mice fed an HFD exhibited higher expression levels of genes related to fatty acid uptake and synthesis (e.g., *Cd36*, *Scd1*, *Pparg*) and lower expression of genes related to fatty acid metabolism (e.g., *Ppara*, *Cpt1a*) (Figure 3I) than Flox mice. *Swap70*-HKO mice displayed more severe liver injury and higher enzyme levels (Figure 3J) (e.g., ALT and AST) than Flox mice. This evidence indicates that SWAP70 deficiency increases susceptibility to insulin resistance and exacerbates HFD-induced NAFLD progression.
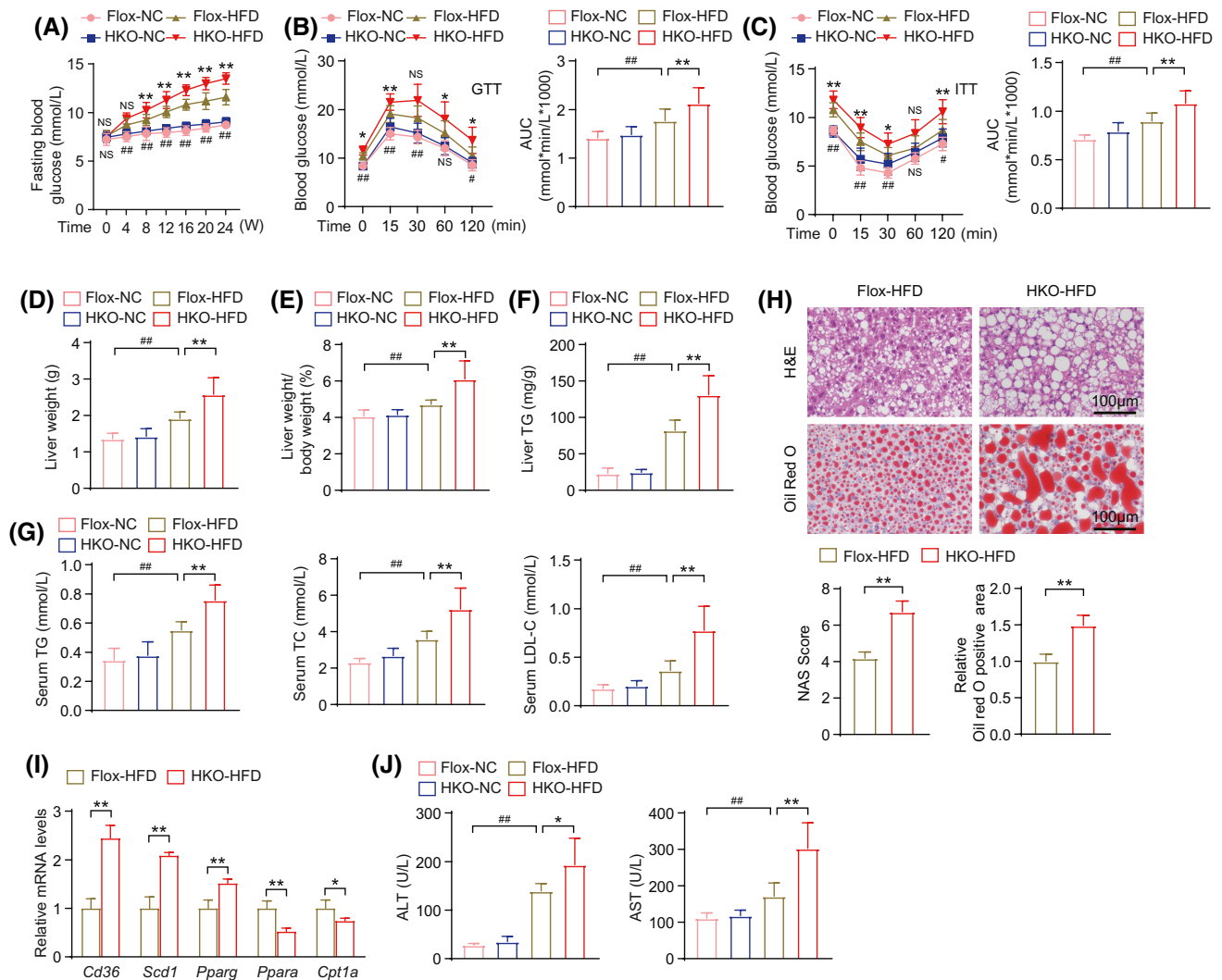
Hepatocyte-specific SWAP70 deficiency exacerbates HFHC diet-induced NASH progression

After HFHC diet feeding for 16 weeks, we examined the body weights of *Swap70*-HKO mice and Flox mice

and found no significant difference between them (Supporting Figure S4A). However, *Swap70*-HKO mice exhibited further increases in FBG levels, liver weights, liver to body weight ratio, and TG levels (Figure 4A-C, Supporting Figure S4B). In the serum, the TG, TC, and LDL-C levels were also higher in *Swap70*-HKO mice than in Flox mice (Figure 4D). Histopathological staining showed increased lipid accumulation in *Swap70*-HKO mice fed an HFHC diet (Figure 4E). Furthermore, *Swap70*-HKO mice exhibited increased CD11b^{+} and Ly6G^{+} inflammatory cells count as well as increased collagen deposition (Figure 4F,G). Consistently, the accumulation of liver enzymes (e.g., ALT and AST) was increased in *Swap70*-HKO mice and induced increased liver injury (Figure 4H). To further systemically evaluate the influence of SWAP70 on the pathogenesis of NASH, we performed RNA-seq on the livers of *Swap70*-Flox and *Swap70*-HKO mice. Cluster analysis showed that the two groups could be clearly separated, indicating a significant difference between them (Supporting Figure S4C). Gene set enrichment analysis showed that *Swap70* deficiency promoted lipid metabolism-related pathways (e.g., fatty acid biosynthetic process, fatty acyl-CoA metabolic process, long chain fatty acid transport, and unsaturated fatty acid biosynthetic process) (Figure 4I, Supporting Figure S4D), inflammatory response-related pathways (e.g., activation of NF-κB inducing kinase activity, positive regulation of chemotaxis, positive regulation of cytokinesis, and positive regulation of inflammatory responses) (Figure 4I, Supporting Figure S4E), fibrosis-related pathways (e.g., complex of collagen trimers, extracellular matrix, and positive regulation of fibroblast proliferation), and gene expression (Figure 4I, Supporting Figure S4F). The heat map displayed the expression pattern of leading edge subsets in livers of *Swap70*-HKO and Flox mice fed the HFHC diet (Figure 4J). Then, we examined some of the representative genes according to the leading edge subsets and confirmed the up-regulation of these genes, including genes related to lipid metabolism (e.g., *Scd1*, *Pparg*), inflammation (e.g., *Tnf*, chemokine [C-X-C motif] 10 [*Cxcl10*], *Ccl2*), and fibrosis (e.g., collagen type III alpha 1 chain, *Tgfb1*) (Figure 4K-M). Collectively, these results demonstrate that hepatocyte-specific SWAP70 deficiency promoted lipid accumulation, inflammation, and fibrosis after HFHC treatment.

SWAP70-OE alleviates HFHC diet-induced NASH progression

We produced *Swap70*-OE mice and verified them by western blotting (Supporting Figure S5A). After 16 weeks on the HFHC diet, we found no obvious differences in body weight between the *Swap70*-OE and control groups (Supporting Figure S5B). However, under the HFHC diet, the *Swap70*-OE group exhibited lower FBG levels, liver TG
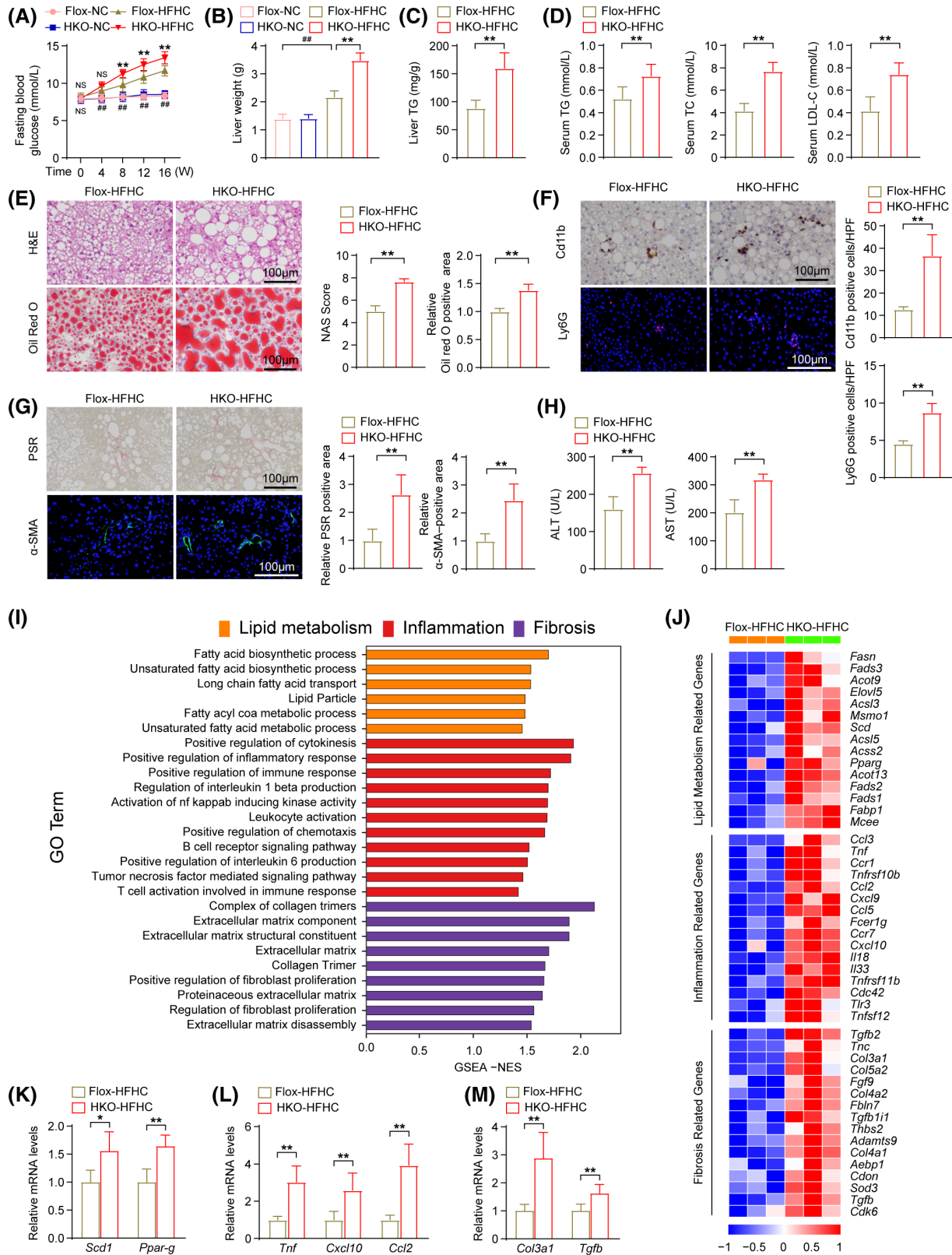
FIGURE 3 Hepatocyte-specific SWAP70 deficiency aggravates exacerbates HFD-induced NAFLD progression. (A) FBG of *Swap70*-Flox and *Swap70*-HKO mice after normal chow (NC) or HFD treatment (*n* = 10-11/group). (B,C) GTT assay and the corresponding AUC of GTT (B); ITT and corresponding AUC (C) of the indicated groups (*n* = 10-11/group). (D,E) Liver weight (D) and liver to body weight ratio (E) of *Swap70*-Flox and *Swap70*-HKO mice after NC or HFD treatment (*n* = 10-11/group). (F) Liver TG contents of *Swap70*-Flox and *Swap70*-HKO mice after NC or HFD treatment (*n* = 10-11/group). (G) Serum TG, TC, and LDL-C level of *Swap70*-Flox and *Swap70*-HKO mice with or without HFD treatment (*n* = 10-11/group). (H) Representative H&E and Oil Red O staining images and quantified results of indicated groups (*n* = 6/group). Scale bars, 100 μm. (I) Relative expression level of genes related to lipid synthesis (*Cd36*, *Scd1*, and *Pparg*) and beta oxidation (*Ppara*, *Cpt1a*) in the liver tissues from indicated groups (*n* = 5/group). (J) Serum ALT and AST contents of the indicated groups (*n* = 10-11/group). Student *t* test (H,I), one-way ANOVA (C-G) with Bonferroni's post hoc analysis or with Tamhane T2 post hoc test or Kruskal-Wallis nonparametric statistical test (A,B,J) was used. All data are shown as mean ± SD. #$p < 0.05$; ##$p < 0.01$ for *Swap70*-Flox mice with NC diet versus HFD. *$p < 0.05$; **$p < 0.01$ for *Swap70*-Flox HFD group versus *Swap70*-HKO HFD group

levels, liver weights, liver to body weight ratio, serum TG, TC, and LDL-C levels compared with control group (Supporting Figure S5C-F). Decreased lipid deposition was observed by H&E and Oil Red O staining in *Swap70*-OE mice, and at the gene level, the opposite changes in lipid synthesis and metabolism genes relative to that of the *Swap70*-deficient mice were shown (Supporting Figure S5G,H). Moreover, CD11b+ and Ly6g+ inflammatory cells and proinflammatory genes (e.g., *Tnf*, *Cxcl2*, *Cxcl10*, and *Ccl2*) were reduced in *Swap70*-OE mice fed an HFHC diet (Supporting Figure S5I,J). Compared with the control group, collagen deposition and the expression of profibrotic genes were also

decreased in the *Swap70*-OE group (Supporting Figure S5K,L), similar to the expression of ALT and AST in the liver (Supporting Figure S5M). These findings demonstrate that SWAP70-OE suppresses the progression of NASH.

SWAP70 alleviates JNK1/2-P38 pathway in mouse livers and hepatocytes in response to metabolic stimulation

To investigate the potential mechanism by which SWAP70 protected against NASH during metabolic

(A) Fasting blood glucose (mmoN/L) vs Time 0 4 8 12 16 (W); Flox-NC, Flox-HFHC, HKO-NC, HKO-HFHC

(B) Liver weight (g); Flox-NC, HKO-NC, Flox-HFHC, HKO-HFHC

(C) Liver TG (mg/g); Flox-HFHC, HKO-HFHC

(D) Serum TG (mmol/L), Serum TC (mmol/L), Serum LDL-C (mmol/L); Flox-HFHC, HKO-HFHC

(E) H&E, Oil Red O; Flox-HFHC, HKO-HFHC; NAS Score; Relative Oil red O positive area

(F) Cd11b, Ly6G; Flox-HFHC, HKO-HFHC; Cd11b positive cells/HPF; Ly6G positive cells/HPF

(G) PSR, α-SMA; Flox-HFHC, HKO-HFHC; Relative PSR positive area; Relative α-SMA-positive area

(H) ALT (U/L), AST (U/L); Flox-HFHC, HKO-HFHC

(I) GO Term — Lipid metabolism, Inflammation, Fibrosis; GSEA −NES

Fatty acid biosynthetic process
Unsaturated fatty acid biosynthetic process
Long chain fatty acid transport
Lipid Particle
Fatty acyl coa metabolic process
Unsaturated fatty acid metabolic process
Positive regulation of cytokinesis
Positive regulation of inflammatory response
Positive regulation of immune response
Regulation of interleukin 1 beta production
Activation of nf kappab inducing kinase activity
Leukocyte activation
Positive regulation of chemotaxis
B cell receptor signaling pathway
Positive regulation of interleukin 6 production
Tumor necrosis factor mediated signaling pathway
T cell activation involved in immune response
Complex of collagen trimers
Extracellular matrix component
Extracellular matrix structural constituent
Extracellular matrix
Collagen Trimer
Positive regulation of fibroblast proliferation
Proteinaceous extracellular matrix
Regulation of fibroblast proliferation
Extracellular matrix disassembly

(J) Flox-HFHC HKO-HFHC; Lipid Metabolism Related Genes: Fasn, Fads3, Acot9, Elovl5, Acsl3, Msmo1, Scd, Acsl5, Acss2, Pparg, Acot13, Fads2, Fads1, Fabp1, Mcee; Inflammation Related Genes: Ccl3, Tnf, Ccr1, Tnfrsf10b, Ccl2, Cxcl9, Ccl5, Fcer1g, Ccr7, Cxcl10, Il18, Il33, Tnfrsf11b, Cdc42, Tlr3, Tnfsf12; Fibrosis Related Genes: Tgfb2, Tnc, Col3a1, Col5a2, Fgf9, Col4a2, Fbln7, Tgfb1i1, Thbs2, Adamts9, Col4a1, Aebp1, Cdon, Sod3, Tgfb, Cdk6

(K) Relative mRNA levels; Scd1, Ppar-g; Flox-HFHC, HKO-HFHC

(L) Relative mRNA levels; Tnf, Cxcl10, Ccl2; Flox-HFHC, HKO-HFHC

(M) Relative mRNA levels; Col3a1, Tgfb; Flox-HFHC, HKO-HFHC

stress, we searched for differentially expressed genes (DEGs) by analyzing RNA-seq obtained from livers of *Swap70*-Flox and *Swap70*-HKO mice (fold change > 1.5 and *p* < 0.05). The results revealed 1,723 DEGs in the livers of *Swap70*-HKO mice compared with the control mice, 872 of which were up-regulated and 851 of which were down-regulated (Figure 5A). Subsequently, we performed Kyoto Encyclopedia of Genes and Genomes analysis based on the DEGs and identified that the MAPK pathway was the most significantly

FIGURE 4 Hepatocyte-specific SWAP70 deficiency exacerbates HFHC diet-induced NASH progression. (A-C) FBG (A), liver weight (B), and liver TG content (C) of *Swap70*-Flox and *Swap70*-HKO mice after normal chow (NC) or HFHC diet (*n* = 9-11/group). (D) Serum TG, TC, and LDL-C level of mice in *Swap70*-Flox and *Swap70*-HKO groups with HFHC diet (*n* = 9-11/group). (E) Representative H&E and Oil Red O staining and quantified results of *Swap70*-Flox and *Swap70*-HKO mice with HFHC diet (*n* = 6/group). (F) Representative immunohistochemical image of CD11b, immunofluorescence image of ly6G, and quantitative results from Image-Pro Plus (*n* = 4-5/group). (G) Representative picrosirius red staining (PSR) and immunofluorescence image of alpha-smooth muscle actin (α-SMA), and quantitative results from Image-Pro Plus (*n* = 4-6/group). (H) Serum ALT (left) and AST (right) contents of the indicated groups (*n* = 4-6/group). (I) Gene set enrichment analysis revealed up-regulated pathways connected to lipid metabolism, inflammation, and fibrosis in livers of the *Swap70*-Flox and *Swap70*-HKO groups. (J) Heatmap shows the leading edge subsets of genes related to lipid metabolism, inflammation, and fibrosis. Genes with a corresponding adjusted *p* value less than 0.05 were considered statistically significant. (K-M) The key molecules related to lipid metabolism (K), inflammation (L), and fibrosis (M) were validated by real-time PCR according to the RNA-seq data (*n* = 6/group). Scale bar, 100 μm. Student *t* test and Mann-Whitney U test(C-H,K-M), one-way ANOVA (B) with Bonferroni's post hoc analysis or with Tamhane T2 post hoc test, or Kruskal-Wallis nonparametric statistical test (A) was used. All data are shown as mean ± SD. ##*p* < 0.01 for *Swap70*-Flox mice with NC diet versus *Swap70*-Flox mice with HFHC diet. *p < 0.05; **p < 0.01 for *Swap70*-Flox HFHC group versus *Swap70*-HKO HFHC group

changed by *Swap70* deficiency (Figure 5B). We examined the activation of MAPK signaling in the livers of *Swap70*-HKO and *Swap70*-OE mice and their respective controls and found that the activation of JNK1/2 and P38 was increased in the livers of *Swap70*-HKO mice, whereas it was suppressed in the livers of *Swap70*-OE mice (Figure 5C,D). However, SWAP70 deficiency or overexpression had no effect on the activation of ERK1/2 (Figure 5C,D). Furthermore, similar results were obtained from the *SWAP70* knockdown and overexpression L02 cells and primary hepatocytes in response to PA stimulation (Figure 5E,F, Supporting Figure S6). Taken together, these results demonstrate that SWAP70 suppresses JNK1/2-P38 activation under metabolic stress.

SWAP70 interacts with TAK1 and inhibits its activation

Considering that SWAP70 suppressed the activation of JNK1/2-P38 signaling in the liver or hepatocytes after metabolic stimulation, we further explored the potential upstream molecules of JNK1/2-P38 signaling regulated by SWAP70. We screened for classical upstream molecules (mitogen-activated protein kinase kinase kinase [MEKK] 1, MEKK2, MEKK3, mitogen-activated protein kinase kinase kinase 5, TAK1, mitogen-activated protein kinase kinase kinase 8, dual specificity mitogen-activated protein kinase kinase [MKK] 4, and MKK7) of the MAPK pathway[21,22] and found that TAK1 showed the strongest interaction with SWAP70 (Figure 6A). Further *in vivo* and *in vitro* experiments showed that SWAP70 suppressed TAK1 phosphorylation under metabolic stress (Figure 6B-E). Immunofluorescence staining revealed the colocalization of SWAP70 and TAK1 in the cytoplasm of HEK 293T cells (Figure 6F). Using exogenous and endogenous immunoprecipitation and GST precipitation assays, we demonstrated that SWAP70 directly interacted with TAK1 (Figure 6G-J). To explore the interaction domain between SWAP70 and TAK1, a molecular mapping assay was used, and we found that

the SWAP70 domain from amino acid (aa) 1-192 interacted with aa 1-306 of TAK1 (Figure 6K,L). Taken together, these results demonstrate that SWAP70 directly interacts with TAK1 and suppresses its activation of under metabolic stimulation.

SWAP70 regulates hepatic steatosis by suppressing the interaction between TAB1 and TAK1

We detected whether the regulation of SWAP70 on TAK1 activity and hepatocyte lipid accumulation was dependent on its interaction with TAK1. We infected hepatocytes with Flag, Flag-*SWAP70*, or Flag-*SWAP70* aa 193-585 plasmids and found that only the full length of SWAP70 could decrease the activation of TAK1 and downstream JNK1/2-P38 pathway and lipid accumulation under metabolic stress (Figure 7A,B). In addition, it is well known that TAB1 is an adaptor protein to TAK1 that binds to the N-terminus of TAK1 and is indispensable for the activation of TAK1.[23] We further investigated whether SWAP70 could affect the interaction of TAB1 and TAK1. The results showed that SWAP70 weakened the interaction between TAB1 and TAK1 and ultimately alleviated the activation of TAK1-JNK1/2-P38 signaling and lipid deposition enhanced by TAB1 (Figure 7C-E). This indicates that SWAP70 may suppress the progression of NAFLD by weakening the interaction between TAB1 and TAK1.

Inhibition of TAK1 activity blocked hepatocyte lipid deposition and inflammation caused by *SWAP70* knockdown

To investigate whether the effect of SWAP70 on hepatocytes lipid accumulation and inflammation was dependent on TAK1 activity, *SWAP70* knockdown or control L02 cells were treated with TAK1 inhibitor 5Z-7 oxozeaenol (5Z-7ox). The results showed that the activation
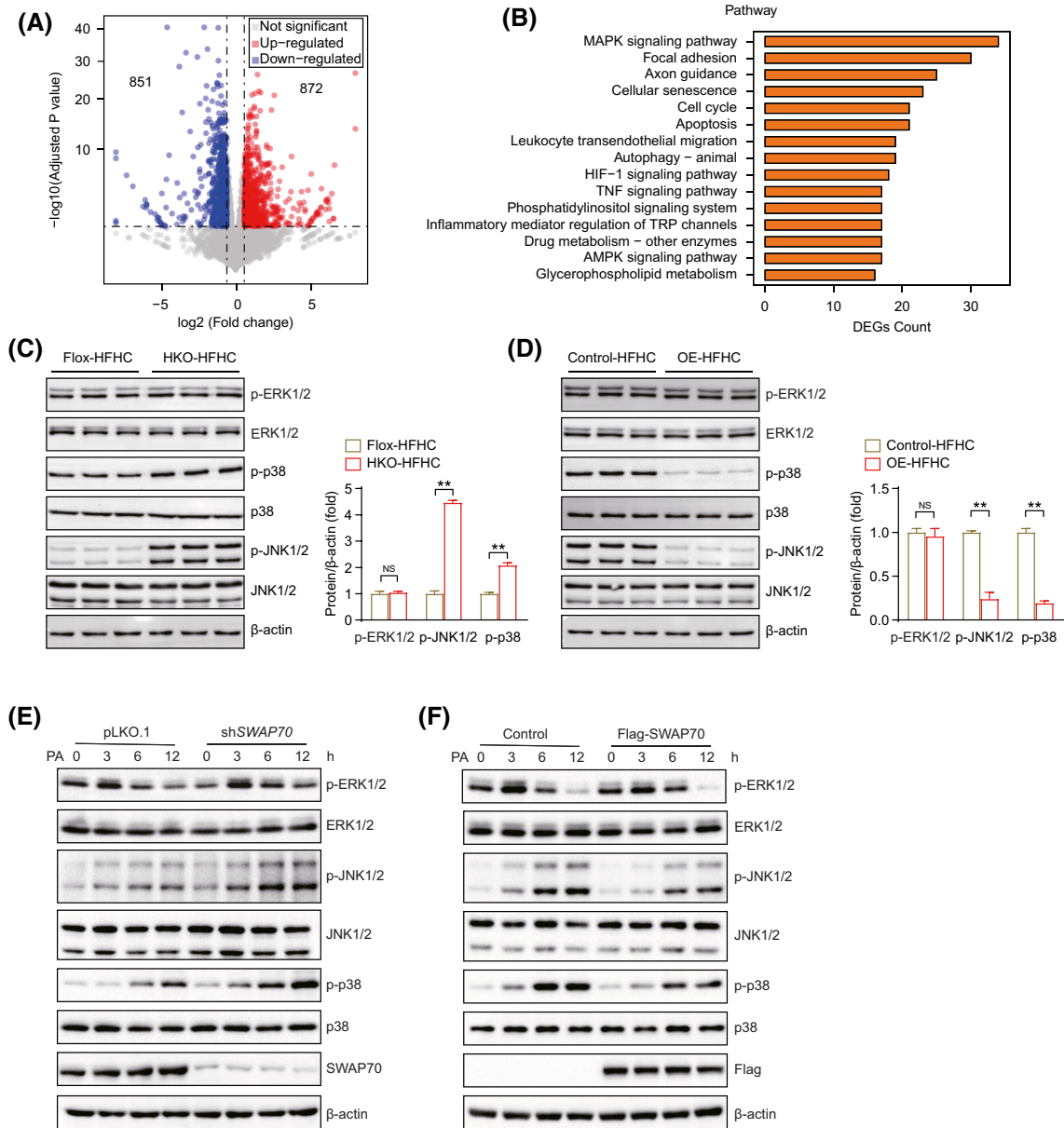
FIGURE 5 SWAP70 inhibits JNK1/2-P38 pathway in mice liver and hepatocytes under metabolic stimulation. (A) Volcano plot showed DEGs in the livers of *Swap70*-Flox or *Swap70*-HKO mice under HFHC treatment. (B) Kyoto Encyclopedia of Genes and Genomes analysis identified most significantly changed pathway according to DEGs. (C) The protein levels of phosphorylated and total ERK1/2, P38, and JNK1/2 in liver tissues from *Swap70*-Flox and *Swap70*-HKO mice with HFHC diet (*n* = 3/group). Quantitative result shown on the right. (D) The protein levels of phosphorylated and total ERK1/2, P38, and JNK1/2 in liver tissues from control and *Swap70*-OE mice with HFHC diet (*n* = 3/group). Quantitative result shown on the right. (E,F) The expression levels of phosphorylated and total ERK1/2, P38, and JNK1/2 in *SWAP70* knockdown (E) or overexpression (F) L02 cells and their control cells under PA stimulation for 0, 3, 6, and 12 hours (*n* = 3 independent experiments). Student *t* test was used. All data are shown as mean ± SD. **p < 0.01

of TAK1 and downstream JNK1/2-P38 induced by *SWAP70* knockdown were blocked by 5Z-7ox treatment (Figure 8A). As expected, elevated hepatocytes lipid accumulation and cellular TG content caused by *SWAP70* knockdown were reversed by 5Z-7ox under PO stimulation (Figure 8B,C). Consistently, *SWAP70* knockdown-induced up-regulation of genes related to lipid synthesis (e.g., *CD36* and *PPARG*) and inflammation (e.g., *IL-6* and *CCL2*) was down-regulated by

5Z-7ox. Simultaneously, the down-regulation of genes related to steatolysis (e.g., *PPARA* and *CPT1A*) induced by *SWAP70* knockdown was blocked by 5Z-7ox (Figure 8D-F). In addition, we silenced the expression of *TAK1* in L02 cells and primary hepatocytes and obtained consistent results with 5Z-7ox (Figure 8G-M, Supporting Figure S7). These results indicated that SWAP70 protects against hepatocyte lipid deposition and inflammation mainly thorough TAK1.
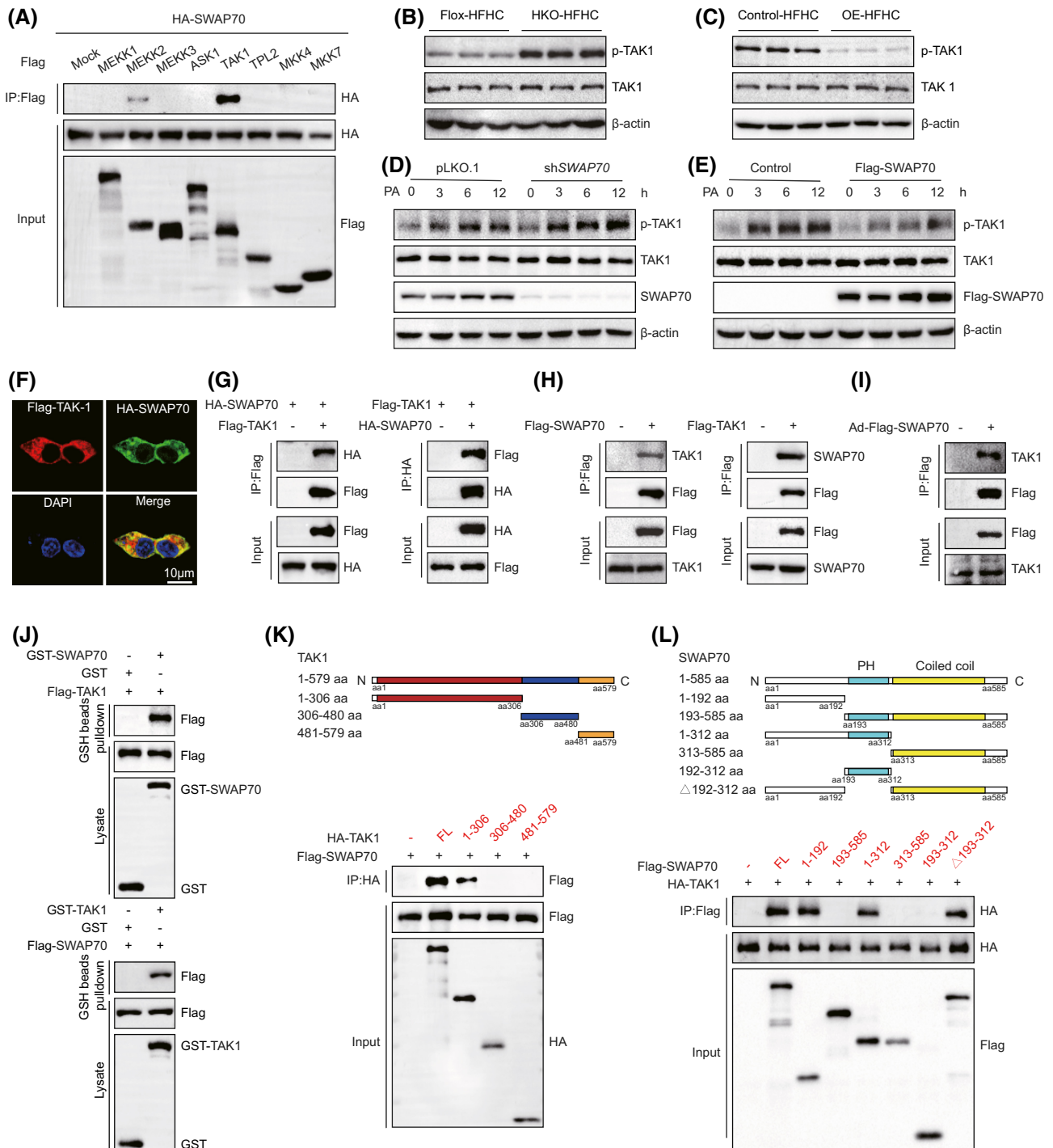
FIGURE 6 SWAP70 interacts with TAK1 and inhibits its activation. (A) Coimmunoprecipitation (CO-IP) assays performed the interaction between Flag-SWAP70 and various upstream molecules of the MAPK pathway ($n = 3$ independent experiments). (B,C) The protein levels of phosphorylated and total TAK1 in liver tissues from indicated groups with HFHC diet ($n = 3$/group). (D,E) Phosphorylated and total TAK1 protein level in L02 cells with *SWAP70* knockdown (D) or overexpression (E) under PA stimulation for 0, 3, 6, or 12 hours ($n = 3$ independent experiments). (F) Colocalization of TAK1 (red) and SWAP70 (green) in HEK 293T cells transfected with Flag-*TAK1* and HA-*SWAP70* plasmids ($n = 3$ independent experiments). Scale bar, 10 μm. (G) CO-IP assay performed the interaction between HA-SWAP70 and Flag-TAK1 in HEK 293T cells ($n = 3$ independent experiments). (H) CO-IP assays performed the interaction between Flag-SWAP70 and endogenous TAK1 or Flag-TAK1 and endogenous SWAP70 in L02 hepatocytes ($n = 3$ independent experiments). (I) CO-IP assays performed the interaction between Flag-SWAP70 and endogenous TAK1 in primary hepatocytes ($n = 3$ independent experiments). (J) GST precipitation assays show direct binding of SWAP70 and TAK1, purified GST as control ($n = 3$ independent experiments). (K) The binding domains of TAK1 and SWAP70 were explored by using Flag-SWAP70 and either full-length or truncated TAK1. Above, schematic diagram of truncated *TAK1*; below, western blot bands (n = 3 independent experiments). (K) The binding domains of SWAP70 and TAK1 were explored using HA-TAK1 and either full-length or truncated SWAP70. Above, schematic diagram of *SWAP70* truncated; below, western blot bands ($n = 3$ independent experiments)
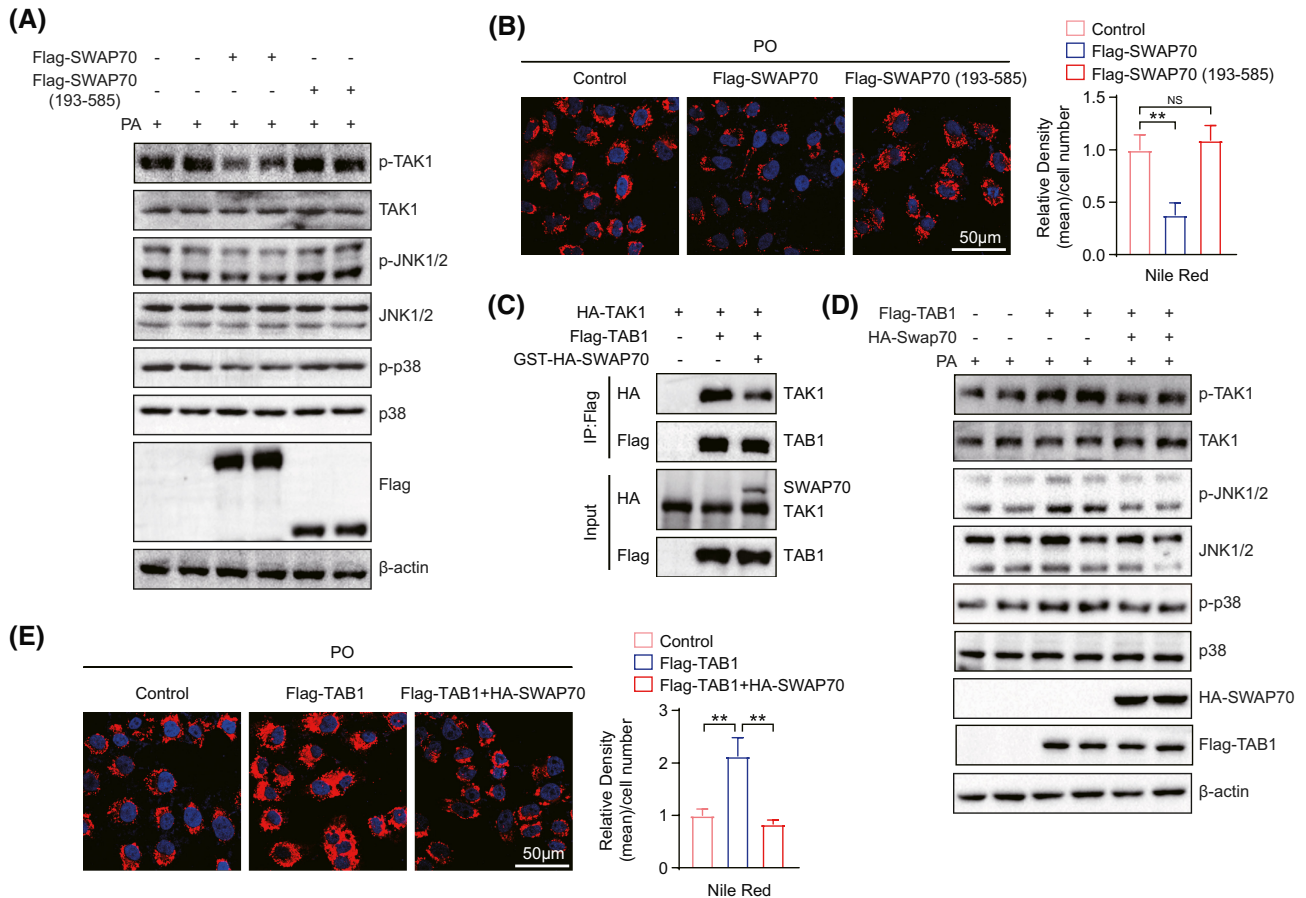
FIGURE 7 SWAP70 regulates hepatic steatosis by suppressing the interaction between TAB1 and TAK1. (A) The expression levels of phosphorylated and total TAK1, JNK1/2, and P38 in L02 cells transfected with Flag, Flag-*SWAP70*, or Flag-*SWAP70* aa 193-585 plasmids with PA stimulation for 12 hours (*n* = 3 independent experiments). (B) Representative Nile Red staining of L02 cells transfected with Flag, Flag-*SWAP70*, or Flag-*SWAP70* aa 193-585 plasmid and quantitative results by Image-Pro Plus (*n* = 3 independent experiments). Scale bar, 50 μm. (C) Coimmunoprecipitation assay showed the interactions among TAB1 and TAK1 in L02 cells transfected with indicated plasmids (*n* = 3 independent experiments). (D) Phosphorylated and total expression levels of TAK1, P38, and JNK1/2 in L02 cells transfected with Flag, Flag-*TAB1*, or Flag-*TAB1* plus HA-*SWAP70* plasmids and stimulated with PA for 12 hours (*n* = 3 independent experiments). (E) Representative Nile Red staining of L02 cells transfected with Flag, Flag-*TAB1*, or HA-*SWAP70* plus Flag-*TAB1* (*n* = 3 independent experiments), quantitative result displayed on right side. Scale bar, 50 μm. One-way ANOVA (A,C) with Bonferroni's post hoc analysis or with Tamhane T2 post hoc test was used. All data are shown as mean ± SD. **p < 0.01

DISCUSSION

Our findings revealed that SWAP70 protected against NASH progression. In a murine model and in hepatocytes experiments, SWAP70-OE in hepatocytes significantly suppressed steatosis in response to metabolic stress. However, this effect was reversed when the expression of SWAP70 was suppressed in hepatocytes. Further experiments showed that SWAP70 interacted with TAK1 and reduced the interaction of TAB1 and TAK1, ultimately suppressing the activation of TAK1 and downstream JNK1/2-P38 signaling. Inhibition of TAK1 activation blocked the detrimental effects of *SWAP70* knockdown on lipid accumulation and inflammatory responses in hepatocytes. These findings suggest that SWAP70 may be a therapeutic target for NAFLD.

Previous studies on SWAP70 have mainly focused on the regulation of immune cells. However, the contribution of SWAP70 to the occurrence and progression of NAFLD is not well understood. Lipid accumulation is an important pathological change in the progression of NAFLD.[24] Compared with convert excess energy into carbon dioxide or very-low-density lipoprotein, liver transformed excess energy into TG more commonly.[25,26] An imbalance in lipid synthesis, transport, and oxidation ultimately leads to a net accumulation of energy in the liver in the form of TGs.[27] Resulting hepatic steatosis beyond the healthy threshold can impair insulin clearance and lead to hepatic lipogenesis and very-low-density lipoprotein oversecretion in patients with NAFLD.[28] Patients with severe steatosis may be more prone to steatohepatitis.[29] Our data demonstrated the role of SWAP70 in lipid metabolism. Under metabolic stress, *Swap70*-HKO mice displayed enhanced lipid deposition and hepatic steatosis.
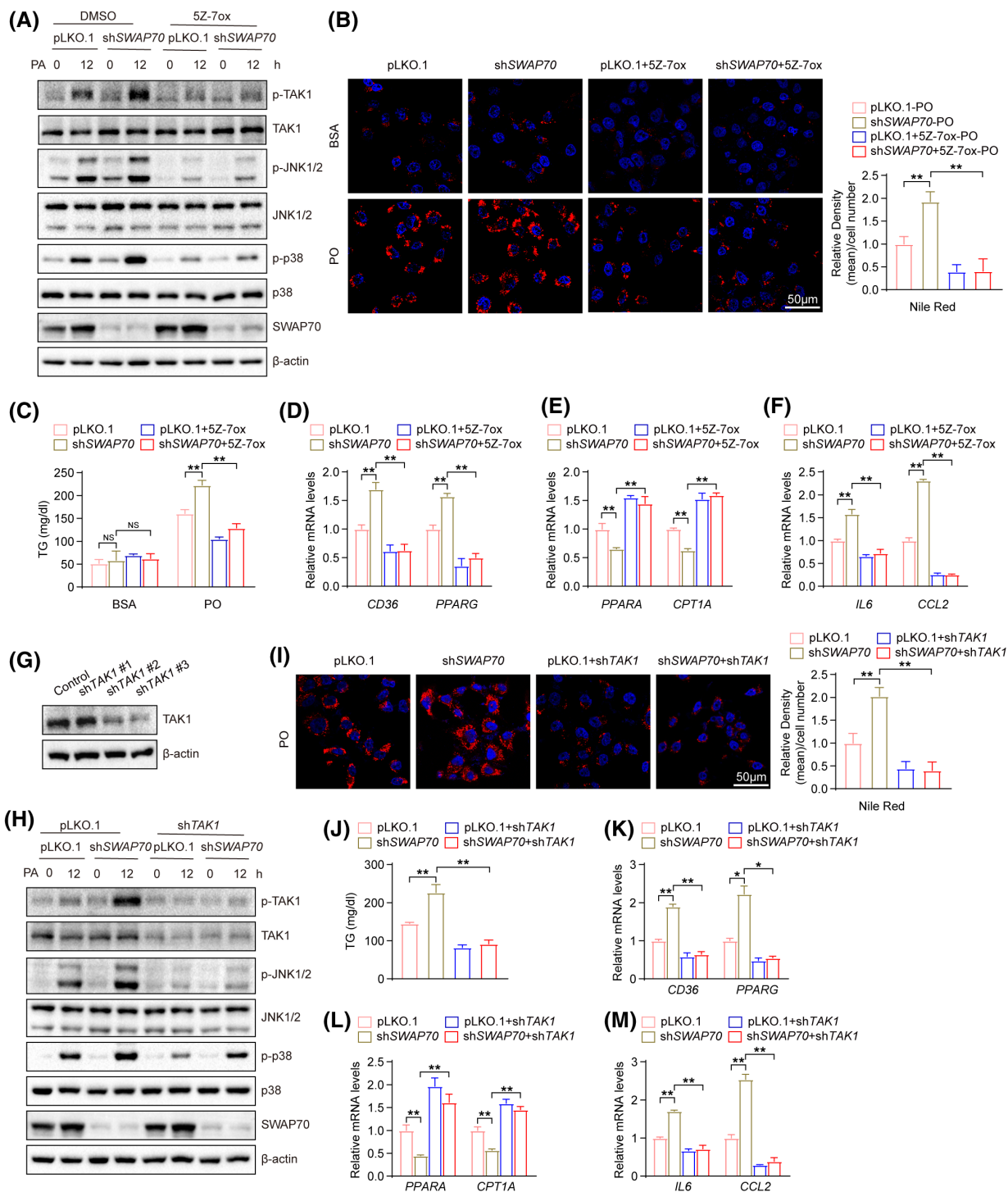
FIGURE 8 TAK1 inhibition blocked hepatocyte lipid deposition and inflammation caused by *SWAP70* knockdown. (A) The expression levels of phosphorylated and total TAK1, JNK1/2, and P38 from the indicated groups (n = 3 independent experiments). (B,C) Representative Nile red staining (B) and relative intracellular TG levels (C) of indicated groups (n = 3 independent experiments); quantified results were performed on the right. (D-F) Relative expression level of genes related to lipid synthesis, β-oxidation, and inflammation in L02 hepatocytes infected with sh*SWAP70* or pLKO.1 lentivirus and then challenged with PA and either 5Z-7ox (100 nM) or dimethylsulfoxide vehicle control (n = 3 independent experiments). (G) Western blot of TAK1 in L02 cells after transfection with pLKO.1, sh*TAK1* #1, sh*TAK1* #2, or sh*TAK1* #3 plasmids. sh*TAK1* #3 was used for further study. (H) The expression levels of phosphorylated and total TAK1, JNK1/2, and P38 from the indicated groups (n = 3 independent experiments). (I) Representative images of Nile Red staining of indicated groups (n = 3 independent experiments). Quantified results were performed on the right. (J) Bar chart showed intracellular TG level of indicated groups (n = 3 independent experiments). (K-M) Relative mRNA expression level of genes related to lipid synthesis, β-oxidation, and inflammation in L02 hepatocytes infected with sh*SWAP70* or pLKO.1 and either sh*TAK1* or pLKO.1 lentivirus and then challenged with PA treatment (n = 3 independent experiments). One-way ANOVA with Bonferroni's post hoc analysis or with Tamhane T2 post hoc test was used. Scale bar, 50 μm. All data are shown as mean ± SD. *$p < 0.05$; **$p < 0.01$

The increased expression of genes related to lipid synthesis and decreased expression of genes related to β-oxidation further demonstrated the protective role of SWAP70 in lipid metabolism.

During the progression of NAFLD, the presence of inflammation can be induced by excess nutrients.[30] The pathogenesis of NAFLD involves the interaction of inflammatory and immune signaling pathways, including inflammasome activation, inflammatory cell responses, and changes in cytokines and chemokines.[25] For example, the IL-1 family cytokines IL-1β, IL-1α, IL-18, and IL-33 can promote NASH.[31] Previous studies have shown that genetic deficiency of *SWAP70* can result in lupus-like symptoms and influence the germinal center formation of B cells.[32,33] Additionally, one study found that the absence of *SWAP70* strongly enhanced the differentiation of dendritic cells.[13] *Swap70*-deficient mice displayed a higher risk of lupus syndrome and accumulation of age-associated B cells.[19] The absence of *SWAP70* has been shown to lead to an immune imbalance in the body and promote the progression of inflammation. These findings are consistent with the inflammatory changes observed in our study. *In vivo* experiments showed that *Swap70*-HKO mice fed an HFHC diet exhibited more severe inflammatory response, increased inflammatory cell infiltration, and increased inflammatory gene expression than control mice. It can be concluded that SWAP70 deficiency further aggravates the inflammatory response in NAFLD and thus promotes its progression.

TAK1 mediates numerous important processes, such as cell death, cell differentiation, immune response, and carcinogenesis.[34,35] The potential role of TAK1 in various diseases, including cardiovascular disease, tumors, and liver metabolic dysfunction, has been well defined.[36-38] Previous studies have shown that the suppression of TAK1 and downstream signaling could significantly improve glycometabolic disorders, lipidosis, inflammation, fibrosis, and tumor formation.[39-41] Hyperactivation of TAK1, on the other hand, can induce hepatic inflammation, metabolic disturbances, and ultimately the progression of NAFLD.[43] Thus, TAK1 homeostasis is vital to liver homeostasis. Recently, TAK1 was shown to regulate the downstream MAPK pathway to mediate the progression of NAFLD.[42] Our findings revealed the interaction between SWAP70 and TAK1 in the screening of upstream molecules of MAPK, confirming that SWAP70 may regulate the progression of NAFLD through TAK1. Consistent with previous studies,[43,44] our findings showed that TAK1 and downstream JNK1/2-P38 signaling are closely interrelated in the progression of NAFLD. Inhibiting the activation of TAK1 and downstream JNK1/2-P38 signaling can therefore suppress the progression of NAFLD. In addition, the loss of aa 1-192 domain of SWAP70 did not improve lipid accumulation in hepatocytes or the activation of TAK1-JNK1/2-P38 signaling, indicating the regulation of SWAP70 on hepatic steatosis is dependent on the interaction between SWAP70 and TAK1. Among the mitogen-activated protein kinase kinase kinase family members, TAK1 is peculiar in its activation mechanism and requires a combination with specific binding proteins known as TAB1, TAB2, and TAB3.[35] As a binding partner protein, TAB1 binds to the N-terminus of TAK1 and is indispensable for its activation.[22] *In vitro* expression of TAB1 can induce autophosphorylation of TAK1 and lead to the activation of TAK1 kinase.[45] Our data revealed that SWAP70 interacts with the N-terminus of TAK1. There may exist an inhibition between SWAP70 and TAB1 in the interaction to TAK1. Similar to our assumption, SWAP70 weakened the interaction between TAK1 and TAB1 and decreased the lipid metabolism and activation of the TAK1-JNK1/2-P38 pathway stimulated by TAB1. Overactivation of TAK1 and the downstream pathway induced by *SWAP70* knockdown, as well as lipid accumulation and inflammation, could be inhibited by the TAK1 inhibitor 5Z-7ox or by silencing of *TAK1*. These results indicate that SWAP70 mainly regulates the progression of NAFLD through TAK1. SWAP70 is a favorable inhibitor of TAK1 phosphorylation and shows potential for the treatment of NAFLD.

In conclusion, the current study shows that SWAP70 may suppress inflammation, lipid storage, fibrosis, and insulin resistance by interfering with the activation of TAK1 and JNK1/2-P38 signaling to protect against the progression of NAFLD. Therefore, SWAP70 may be a potential therapeutic target for NAFLD.

CONFLICT OF INTEREST
The authors declare no competing interests.

AUTHOR CONTRIBUTIONS

ORCID
Manli Hu https://orcid.org/0000-0001-8318-0454

REFERENCES
1. Estes C, Anstee QM, Arias-Loste MT, Bantel H, Bellentani S, Caballeria J, et al. Modeling NAFLD disease burden in China, France, Germany, Italy, Japan, Spain, United Kingdom, and United States for the period 2016–2030. J Hepatol. 2018;69(4):896–904.
2. Huang DQ, El-Serag HB, Loomba R. Global epidemiology of NAFLD-related HCC: trends, predictions, risk factors and prevention. Nat Rev Gastroenterol Hepatol. 2021;18(4):223–38.

3. Bence KK, Birnbaum MJ. Metabolic drivers of non-alcoholic fatty liver disease. Mol Metab. 2020;50:101143.

4. Younossi Z, Stepanova M, Ong JP, Jacobson IM, Bugianesi E, Duseja A, et al. Nonalcoholic steatohepatitis is the fastest growing cause of hepatocellular carcinoma in liver transplant candidates. Clin Gastroenterol Hepatol. 2019;17(4):748–55.e3.

5. Zhou F, Zhou J, Wang W, Zhang XJ, Ji YX, Zhang P, et al. Unexpected rapid increase in the burden of NAFLD in China from 2008 to 2018: A systematic review and meta-analysis. Hepatology. 2019;70(4):1119–33.

6. Li J, Zou B, Yeo YH, Feng Y, Xie X, Lee DH, et al. Prevalence, incidence, and outcome of non-alcoholic fatty liver disease in Asia, 1999–2019: a systematic review and meta-analysis. Lancet Gastroenterol Hepatol. 2019;4(5):389–98.

7. Ramadan MS, Russo V, Nigro G, Durante-Mangoni E, Zampino R. Interplay between heart disease and metabolic steatosis: a contemporary perspective. J Clin Med. 2021;10(8):1569.

8. Targher G, Byrne CD, Tilg H. NAFLD and increased risk of cardiovascular disease: clinical associations, pathophysiological mechanisms and pharmacological implications. Gut. 2020;69(9):1691–705.

9. Chen ZE, Liu J, Zhou F, Li H, Zhang XJ, She ZG, et al. Nonalcoholic fatty liver disease: an emerging driver of cardiac arrhythmia. Circ Res. 2021;128(11):1747–65.

10. Baranov MV, Revelo NH, Dingjan I, Maraspini R, ter Beest M, Honigmann A, et al. SWAP70 organizes the actin cytoskeleton and is essential for phagocytosis. Cell Rep. 2016;17(6):1518–31.

11. Betaneli V, Jessberger R. Mechanism of control of F-actin cortex architecture by SWAP-70. J Cell Sci. 2020;133(2):jcs233064.

12. Shinohara M, Terada Y, Iwamatsu A, Shinohara A, Mochizuki N, Higuchi M, et al. SWAP-70 is a guanine-nucleotide-exchange factor that mediates signalling of membrane ruffling. Nature. 2002;416(6882):759–63.

13. Popovic J, Wellstein I, Pernis A, Jessberger R, Ocana-Morgner C. Control of GM-CSF-dependent dendritic cell differentiation and maturation by DEF6 and SWAP-70. J Immunol. 2020;205(5):1306–17.

14. Shi L, Liu H, Wang Y, Chong Y, Wang J, Liu G, et al. SWAP-70 promotes glioblastoma cellular migration and invasion by regulating the expression of CD44s. Cancer Cell Int. 2019;19(1):305.

15. Ocana-Morgner C, Gotz A, Wahren C, Jessberger R. SWAP-70 restricts spontaneous maturation of dendritic cells. J Immunol. 2013;190(11):5545–58.

16. Pearce G, Audzevich T, Jessberger R. SYK regulates B-cell migration by phosphorylation of the F-actin interacting protein SWAP-70. Blood. 2011;117(5):1574–84.

17. Garbe AI, Roscher A, Schüler C, Lutter AH, Glösmann M, Bernhardt R, et al. Regulation of bone mass and osteoclast function depend on the F-actin modulator SWAP-70. J Bone Miner Res. 2012;27(10):2085–96.

18. Biswas PS, Gupta S, Stirzaker RA, Kumar V, Jessberger R, Lu TT, et al. Dual regulation of IRF4 function in T and B cells is required for the coordination of T-B cell interactions and the prevention of autoimmunity. J Exp Med. 2012;209(3):581–96.

19. Manni M, Gupta S, Ricker E, Chinenov Y, Park SH, Shi M, et al. Regulation of age-associated B cells by IRF5 in systemic autoimmunity. Nat Immunol. 2018;19(4):407–19.

20. Ji YX, Wang Y, Li PL, Cai L, Wang XM, Bai L, et al. A kinome screen reveals that Nemo-like kinase is a key suppressor of hepatic gluconeogenesis. Cell Metab. 2021;33(6):1171–86.e9.

21. Huang G, Shi LZ, Chi H. Regulation of JNK and p38 MAPK in the immune system: signal integration, propagation and termination. Cytokine. 2009;48:161–9.

22. Xu D, Matsumoto ML, McKenzie BS, Zarrin AA. TPL2 kinase action and control of inflammation. Pharmacol Res. 2018;129:188–93.

23. Roh YS, Song J, Seki E. TAK1 regulates hepatic cell survival and carcinogenesis. J Gastroenterol. 2014;49(2):185–94.

24. Kořínková L, Pražienková V, Černá L, Karnošová A, Železná B, Kuneš J, et al. Pathophysiology of NAFLD and NASH in experimental models: the role of food intake regulating peptides. Front Endocrinol (Lausanne). 2020;11:597583.

25. Loomba R, Friedman SL, Shulman GI. Mechanisms and disease consequences of nonalcoholic fatty liver disease. Cell. 2021;184(10):2537–64.

26. Mashek DG. Hepatic lipid droplets: a balancing act between energy storage and metabolic dysfunction in NAFLD. Mol Metab. 2021;50:101115.

27. Heeren J, Scheja L. Metabolic-associated fatty liver disease and lipoprotein metabolism. Mol Metab. 2021;50:101238.

28. Bril F, Lomonaco R, Orsak B, Ortiz-Lopez C, Webb A, Tio F, et al. Relationship between disease severity, hyperinsulinemia, and impaired insulin clearance in patients with nonalcoholic steatohepatitis. Hepatology. 2014;59(6):2178–87.

29. Chalasani N, Wilson L, Kleiner DE, Cummings OW, Brunt EM, Unalp A. Relationship of steatosis grade and zonal location to histological features of steatohepatitis in adult patients with non-alcoholic fatty liver disease. J Hepatol. 2008;48(5):829–34.

30. Cai D, Yuan M, Frantz DF, Melendez PA, Hansen L, Lee J, et al. Local and systemic insulin resistance resulting from hepatic activation of IKK-beta and NF-kappaB. Nat Med. 2005;11(2):183–90.

31. Mirea AM, Tack CJ, Chavakis T, Joosten L, Toonen E. IL-1 family cytokine pathways underlying NAFLD: towards new treatment strategies. Trends Mol Med. 2018;24(5):458–71.

32. Chandrasekaran U, Yi W, Gupta S, Weng C-H, Giannopoulou E, Chinenov Y, et al. Regulation of effector treg cells in murine lupus. Arthritis Rheumatol. 2016;68(6):1454–66.

33. Quemeneur L, Angeli V, Chopin M, Jessberger R. SWAP-70 deficiency causes high-affinity plasma cell generation despite impaired germinal center formation. Blood. 2008;111(5):2714–24.

34. Ajibade AA, Wang HY, Wang RF. Cell type-specific function of TAK1 in innate immune signaling. Trends Immunol. 2013;34(7):307–16.

35. Aashaq S, Batool A, Andrabi KI. TAK1 mediates convergence of cellular signals for death and survival. Apoptosis. 2019;24(1-2):3–20.

36. Brenner C, Galluzzi L, Kepp O, Kroemer G. Decoding cell death signals in liver inflammation. J Hepatol. 2013;59(3):583–94.

37. Mukhopadhyay H, Lee NY. Multifaceted roles of TAK1 signaling in cancer. Oncogene. 2020;39(7):1402–13.

38. Liu W, Wang G, Zhang C, Ding W, Cheng W, Luo Y, et al. MG53, a novel regulator of KChIP2 and $I_{to,f}$, plays a critical role in electrophysiological remodeling in cardiac hypertrophy. Circulation. 2019;139(18):2142–56.

39. Tan S, Zhao J, Sun Z, Cao S, Niu K, Zhong Y, et al. Hepatocyte-specific TAK1 deficiency drives RIPK1 kinase-dependent inflammation to promote liver fibrosis and hepatocellular carcinoma. Proc Natl Acad Sci U S A. 2020;117(25):14231–42.

40. Bettermann K, Vucur M, Haybaeck J, Koppe C, Janssen J, Heymann F, et al. TAK1 suppresses a NEMO-dependent but NF-kappaB-independent pathway to liver cancer. Cancer Cell. 2010;17(5):481–96.

41. Inokuchi S, Aoyama T, Miura K, Osterreicher CH, Kodama Y, Miyai K, et al. Disruption of TAK1 in hepatocytes causes hepatic injury, inflammation, fibrosis, and carcinogenesis. Proc Natl Acad Sci U S A. 2010;107(2):844–9.

42. Ji YX, Huang Z, Yang X, Wang X, Zhao LP, Wang PX, et al. The deubiquitinating enzyme cylindromatosis mitigates nonalcoholic steatohepatitis. Nat Med. 2018;24(2):213–23.

43. Wu L, Liu Y, Zhao Y, Li M, Guo L. Targeting DUSP7 signaling alleviates hepatic steatosis, inflammation and oxidative stress in high fat diet (HFD)-fed mice via suppression of TAK1. Free Radic Biol Med. 2020;153:140–58.

44. Wu YK, Hu LF, Lou DS, Wang BC, Tan J. Targeting DUSP16/TAK1 signaling alleviates hepatic dyslipidemia and inflammation

in high fat diet (HFD)-challenged mice through suppressing JNK MAPK. Biochem Biophys Res Commun. 2020;524(1):142–9.

45. Kishimoto K, Matsumoto K, Ninomiya-Tsuji J. TAK1 mitogen-activated protein kinase kinase kinase is activated by autophosphorylation within its activation loop. J Biol Chem. 2000;275(10):7359–64.

SUPPORTING INFORMATION

Additional supporting information may be found in the online version of the article at the publisher's website.